

**VENTILATION AND COOLING**  
**18TH ANNUAL AIVC CONFERENCE**  
**ATHENS, GREECE, 23-26 SEPTEMBER 1997**

**Title:** Airflow through Horizontal Openings

Stairwell

**Authors:** A.A.Peppes , M. Santamouris and D.N.Asimakopoulos

**Affiliation:** Group Building Environmental Studies, Physics Dept.,  
University of Athens, University Campus 15784, Athens, Greece.

## Airflow through Horizontal Openings

A.A.Peppes , M. Santamouris and D.N.Asimakopoulos  
Group Building Environmental Studies  
Department of Applied Physics, University of Athens,  
Building PHYS-V, Athens 15784, Greece

**Synopsis** - This paper deals with the interzonal air movement in a building, through horizontal openings, under natural convective conditions. These airflow phenomena are investigated experimentally, through a series of experiments in the stairwell of a full-scale building, using tracer gas technique. The resulting time-dependent concentration evolution offers a means of analyzing the flow field. These cases are also simulated by a CFD code, that uses the finite-volume method and incorporates a low-Reynolds  $k$ - $\epsilon$  two equation turbulence model. The simulations results regarding the concentration and velocity, are in good agreement with experimental data. Results indicate that the contaminant transmission and consequently the airflow pattern is quite complex and is affected by geometry, location of heat and contaminant sources, building materials and microclimate. The study also discusses the effectiveness of CFD modeling to describe airflow phenomena through horizontal openings, under various conditions. The results could be used to develop accurate algorithms for inclusion in existing mathematical models.

### List of Symbols

$d$ = distance from the nearest wall(m)	$u,v,w$ = velocity components ( $\text{msec}^{-1}$ )
$g$ = acceleration due to gravity ( $\text{msec}^{-2}$ )	$x,y,z$ = spatial coordinates
$G_k$ =stress production of turb.kin.energy	$\alpha$ = thermal diffusivity ( $\text{m}^2 \text{sec}^{-1}$ )
$G_B$ =buoyant generation of turb.kin.energy	$\beta$ = coefficient of thermal expansion( $\text{K}^{-1}$ )
$H$ = height of the stairwell (m)	$\Gamma_\phi$ = exchange coefficient of $\phi$
$k$ =kin.energy of turbulence( $\text{Jkg}^{-1}$ )	$\epsilon$ =dissipation rate of kin.energy( $\text{Jkg}^{-1}\text{sec}^{-1}$ )
$p$ = pressure (Pa)	$\mu_e$ =effective dynamic viscosity( $\text{kgm}^{-1}\text{sec}^{-1}$ )
$Ra$ = Rayleigh number (dimensionless)	$\mu_t$ =turb.dynamic viscosity( $\text{kgm}^{-1}\text{sec}^{-1}$ )
$T$ = temperature (K)	$\rho$ = density ( $\text{kgm}^{-3}$ )
$T_o$ = reference temperature (K)	$\sigma$ = turb.Schmidt or Prandtl number
$t$ = time (sec)	$\phi$ = dependent variable

### 1. Introduction

In recent years there has been an increased interest in the study of airflow through large internal openings. This issue is of great importance due to its implication on energy saving, adequate ventilation, thermal comfort, pollutant transfer and dispersion of fire and smoke in the interior of buildings. However, little work has been done on the airflow through horizontal openings, such as ventilation shafts and stairwells. Indeed, very few authors have studied these phenomena and very few systematic experimental data are available in the literature.

A number of studies have been reported. Brown [1] have investigated airflow through small square openings in horizontal partitions. Reynolds [2], Zohrabian et al.[3] have

conducted experiments and developed a model for the energy and mass transfer in a stairwell model, Riffat et al [5] has studied buoyancy-driven flow through a staircase in a two-floor house. In other studies Zohrabian et al.[4], S.Ergin-Ozkan et al. [7] and Riffat [6] used CFD modeling and compared predictions with experimental data.

There are studies involving air flow prediction in rooms (Haghighat et al. [8], Murakami et al. [9]), in atriums (Alamdari et al.[10]) and others involving measurements and CFD modeling of contaminant transmission in indoor spaces (Drangsholt [11], Subrata et al.[12]).

Recent research in Computational Fluid Dynamics and tracer gas measurement permit to analyze these airflow phenomena, conducting extensive modeling.

The purpose of this study is to expand the existing knowledge on the physical phenomena related to natural convection in a stairwell and on the other hand to compare the CFD predictions and measurements and consequently to provide foundations for improving the existing predictive procedures.

## 2. Description of Experiments

A series of experiments have been performed in a building, in order to study the buoyancy-driven airflow between floors. Five experiments were held at the main stairwell located in the central building of the Department of Applied Physics of University of Athens. The stairwell extends to a height of about 16.5m as it connects the four floors of the building and a small basement. Each floor is about 3.7m high, while the basement is about 1.7m high. Since the geometry is rather complex, figures can describe the building in a more effective way. Figure 1, shows a section of the specific experimental site, while Figure 2 depicts a horizontal plan, which is identical for all floors, since the internal design is common. The rest of dimensions are illustrated in these figures. The entrance door, the doors connecting the stairwell with the offices located in the four floors and all the windows were kept closed and sealed during all the experiments. Some small openings and cracks were also sealed in order to reduce the infiltration as much as possible.

The thermal performance of the stairwell was constantly monitored. The air temperature was monitored by five Tiny Tag sensors (accuracy:  $\pm 0.6\%$ ) which had already been calibrated. These sensors were distributed, one on each floor, and placed in specific locations which remained the same for all the experiments (Figure 1,2). Surface temperature on almost all the internal surfaces, was measured by PT100 sensors (accuracy:  $\pm 0.1\%$ ). Air velocity measurements were also provided by two Dantec sensors (accuracy:  $\pm 0.4\%$ ), located in two specific points of the stairwell for all the experiments (Figure 1,2).

A single tracer gas technique was adopted. Several tracer gases are available, but  $N_2O$  was chosen for this work since it has desirable characteristics in terms of detectability, safety and cost and it has been used successfully in previous air movement studies. The concentration of gas was measured using an infrared gas analyzer (accuracy:  $\pm 1\%$ ). The tracer gas was injected in a specific position via three (3) injection points placed altogether, and eight (8) sampling points were carefully chosen and distributed so as to monitor its concentration variation with time at various heights of the stairwell. Samples were taken every 30 seconds for the total duration of each experiment.

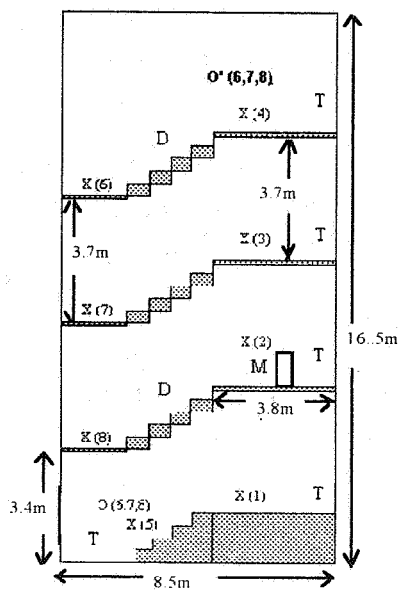


Fig. 1. Section of the stairwell. (1m from the facade of building). Location of injection and sampling points and sensors for all the experiments: X (sampling point), O (injection point for A,B,D exper.), O' (injection point for C,E exper.), M (main unit), T (air temp. sensor) D ( air velocity sensor).

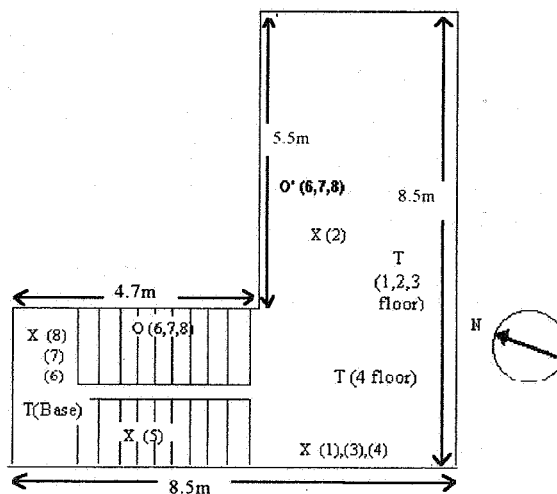


Fig. 2. Horizontal plan of the stairwell (2m from the facade of building). Location of injection and sampling points and sensors for all the experiments: X (sampling point), O (injection point for A,B,D exper.), O' (injection point for C,E exper.), M (main unit), T (air temp. sensor) D ( air velocity sensor).

Five experiments were carried out during January and February of this year, as it was mentioned before. From now on, they will be referred as experiment A, B, C, D, E. The duration of monitoring of gas concentration for each experiment was 75, 95, 75, 60, 58 minutes, respectively. In the first three experiments (A,B,C), monitoring of concentration at sampling points started as soon as the gas injection finished. For the experiments A and B, the gas was released in a specific position in the basement, while for experiment C, the injection took place in the fourth floor (Figures 1,2).

In the other experiments (D and E), the concentration of gas was monitored as soon as the gas release initialized, provided that the gas injection rate was nearly constant for the whole duration of experiments. This rate was initially measured by a flow-meter for an almost constant pressure level as written down on the display of main unit. Its value remained around  $0.00030 \text{ kg gas m}^{-3}$  for the D and E experiments.

For experiment D, the gas was injected in the basement, in the same position as in experiments A and B, while for experiment E, the release took place in the fourth floor, in the same position as in experiment C (Fig. 1,2). The positions of sampling points were the same for all the experiments and for the total durations (Fig. 1,2).

### 3. Description of Numerical Computation

**Mathematical Model** - The mathematical model was a CFD code that generate approximate solutions to the Navier-Stokes equations, which are considered universally valid to describe the flow of a fluid, heat and concentration in a specific field. These equations are based on the conservation equations of mass, momentum, thermal energy and concentration species.

For Rayleigh numbers higher than  $10^6$ , a two equation k-ε model of turbulence was employed [13,14]. Since Rayleigh numbers were ranging from  $3 \cdot 10^{12}$  to  $4 \cdot 10^{12}$  during all the experiments, turbulence calculations were necessary to predict the flow. These equations can be represented by a general form of a differential equation for the dependent variable  $\phi$  :

$$-\frac{\partial}{\partial t}(\rho\phi) + \frac{\partial}{\partial x}(\rho u\phi) + \frac{\partial}{\partial y}(\rho v\phi) + \frac{\partial}{\partial z}(\rho w\phi) = -\frac{\partial}{\partial x}\left(\Gamma_\phi \frac{\partial \phi}{\partial x}\right) + \frac{\partial}{\partial y}\left(\Gamma_\phi \frac{\partial \phi}{\partial y}\right) + \frac{\partial}{\partial z}\left(\Gamma_\phi \frac{\partial \phi}{\partial z}\right) + S_\phi \quad (1)$$

where the first term stands for transience, the remaining three terms in the left part of equation represent convection, the first three terms on the right part stand for diffusion ( $\Gamma_\phi$  stands for diffusivity for scalar variables and for effective viscosity  $\mu_e$  for velocities) and finally  $S_\phi$  gives the source rate. It is obvious that  $\phi$  can be any scalar variable (such as enthalpy  $h$ , kinetic energy  $k$ , energy dissipation  $\epsilon$ , concentration  $c$ ) or vector variable ( $u, v, w$  velocities components). Its value is equal to 1 for the continuity equation. The turbulent dynamic viscosity was determined as :

$$\mu_t = C_\mu \rho k^2 / \epsilon \quad (2)$$

where  $C_\mu$  is determined experimentally. The standard k-ε model can obtain satisfactory results for forced convection configurations - high Reynolds number- as it incorporates the "wall function" method to bridge the rapid variations of velocity and temperature near the wall. The advantage of this approach is its computational economy as it eliminates the need for considering many grid points in the region near the wall.

Unfortunately, such wall laws are not adapted to natural convection problems as this specific one [15]. Therefore the viscous sublayer must be discretized and the behavior of turbulent variables must be damped within the whole domain through low-Reynolds modeling. The low-Reynolds extension of Lam and Bremhorst [16] to the two equation k-ε model, was used here. According to this model the empirical constants  $C_\mu$  in the calculation of turbulent viscosity  $\mu_t$  (equation (2)) and  $C_1, C_2$  constants appearing in the source term of conservation equation of dissipation rate  $\epsilon$ , were multiplied respectively by the functions :

$$F_\mu = [1 - \exp(-0.0165 R_k)]^2 (1 + 20.5 / R_t) \quad (3)$$

$$F_1 = 1 + (0.05 / F_\mu)^3 \quad (4)$$

$$F_2 = 1 - \exp(-R_t^2) \quad (5)$$

where  $R_k = k^2 / (v \epsilon)$  and  $R_t = k^{0.5} d / v$  are the turbulence Reynolds numbers and  $d$  is the distance to the nearest wall. For high Reynolds numbers  $F_\mu, F_1, F_2$  tend to unity.

Separating and reattaching flow regions may occur in buildings which extend in height and have quite complex geometry. Yap [17] proposed an additional source term to the  $\epsilon$  equation which takes into account these phenomena so as to avoid prediction of excessive heat transfer coefficient in such regions. His correction was also applied in these simulations.

**Solution Procedure** - The numerical resolution procedure of the calculations which couple the pressure, velocities, temperature and turbulent variables was the SIMPLE algorithm

(Semi-Implicit Method for Pressure Linked Equations) developed by Patankar [18]. The governing equations were spatially discretized over a 'staggered' grid using the Finite Volume Method (FVM). The Power-Law differencing which gives physically realistic solutions even for coarse grids, was used for the convective-diffusive fluxes and the source terms were linearized. These equations were solved using the line-by-line Tri-diagonal Matrix Algorithm (TDMA).

For the transient approach, the Fully Implicit Scheme was adopted [18]. This scheme does not dictate any restrictions on the time-interval selection, as other schemes do, and satisfies generally the common requirements for simplicity and physical behavior. For the boundary conditions, the non-slip condition at the solid surfaces was applied for velocities. The  $k$  was zero at the solid surfaces and the gradient of  $\epsilon$  normal to the surfaces was considered zero. The temperature of the surfaces were taken from the measurements and considered constant for the duration of experiments.

The results were obtained for a  $52 \times 42 \times 92$  ( $x$ -,  $y$ - and  $z$ -directions, respectively) grid size. Since low-Reynolds number modeling requires that the equations are integrated right down to the wall, care was taken to ensure good numerical resolution in the near-wall region. So a non-uniform grid was adopted. Indeed, nearly five grid points were located in the region  $y^+ < 11.5$  where the laminar sublayer exists, with the first node positioned at  $y^+ = 1.0$ , where  $y^+ = u_T d_p / \nu$  is the dimensionless distance from the surfaces and  $u_T = \sqrt{\tau_w / \rho}$  is the friction velocity, while  $d_p$  is the distance of point P from the wall and  $\nu$  is the kinematic viscosity. A similar approach is to concentrate several grid points inside the wall boundary layer. Its thickness  $\delta$  is estimated by the relation  $\delta/H = 4.86 Ra^{-0.25}$  (6) with the first point located very close to the wall ( $y/H = 10^{-6}$ ) [13]. To conclude, dense grid was put near walls and other solid surfaces -although it was particularly difficult because of the presence of the stairs- for the selected grid size, and a relatively coarse grid arrangement in other regions. Negligible changes to the variables ( $\sim 1\%$ ) were found when a larger grid size was adopted. However it is very significant to obtain results with sufficient accuracy, while achieving the best computational economy at the same time.

The criterion for convergence for all dependent variables was the following:

$\max |\phi^{n+1} - \phi^n| \leq 10^{-4}$  between two successive sweeps. At this stage the sum of the mass residuals had to be less than a small value ( $10^{-3} \text{ kgr sec}^{-1}$ ). The convergence becomes quite problematic in low-Reynolds number flows. Therefore, strong under-relaxation was used - false Dt type - for all the variables, except pressure [18]. Variable relaxation factors were applied during simulations in order to achieve convergence earlier.

#### 4. Results and Discussion

Simulations of the cases corresponding to the five experiments, described before, were carried out. Care was taken to provide the initial field values for the concentration and temperature which are necessary for the simulations.

For the cases corresponding to the A,B,C experiments, the concentration levels measured at the various points just when the gas release finished, were considered as the initial values dominated in each zone-floor. For the rest of cases (D and E experiments) the concentration was considered zero for the whole domain with the existence of a static production source characterized by an almost constant injection rate. In a similar way, the initial values of temperature for each zone were taken from the measurements just the moment the

monitoring started. The average value and the standard deviation of temperature for each floor are presented in Table 1 :

Table 1. Average air temperature (°C)

Air Temp. (°C)	Exper. 1	Exper. 2	Exper. 3	Exper. 4	Exper. 5
Basement	11.18 ± 0.10	11.62 ± 0.09	9.45 ± 0.13	11.07 ± 0.08	9.30 ± 0.01
Floor 1	15.82 ± 0.23	16.18 ± 0.13	14.99 ± 0.16	16.14 ± 0.10	14.40 ± 0.18
Floor 2	17.28 ± 0.19	17.26 ± 0.24	15.49 ± 0.16	17.26 ± 0.19	14.89 ± 0.23
Floor 3	16.80 ± 0.19	17.11 ± 0.18	15.20 ± 0.18	16.80 ± 0.09	14.50 ± 0.25
Floor 4	17.82 ± 0.31	18.02 ± 0.14	16.63 ± 0.13	18.11 ± 0.11	16.02 ± 0.23

The temperature in each floor changed insignificantly with time. The relatively short duration of the experiments is the main cause. Comparison of data with the simulation predictions showed an average value of relative difference of about 2-3%. The greater values were measured on the fourth floor. This was expected, due to the buoyant motions and the fact that the air on the highest floor came to contact with warmer surfaces.

From the analysis of air velocity measurements at the two specific points in the staircase (ranging from 0.05 to 0.15 m sec<sup>-1</sup>) and their comparison with the simulation results (ranging from 0.01 to 0.11 m sec<sup>-1</sup>), it was observed an underestimation of values as calculated from the model. The air motion was rather weak due mainly, to the temperature distribution. The air velocity measurements were very limited in order to give a more detailed description of airflow. However, the simulations gave the overall features of flow patterns. Several vortexes were identified. These eddies promoted the heat transfer and the uniformity of temperature within each floor. The complex geometry of the stairwell produced a strong three-dimensional flow.

Comparison of the measured concentration evolution at all monitoring points with the model predicted one, showed relatively good agreement. The average value of relative difference with its standard deviation and the correlation coefficient for each experiment are presented in Table 2 :

Table 2. Average Relative Difference of Concentration levels

	Exper. 1	Exper. 2	Exper. 3	Exper. 4	Exper. 5
Rel.Differ.	0.12 ± 0.09	0.14 ± 0.10	0.24 ± 0.18	0.18 ± 0.14	0.22 ± 0.20
Corr.Coeff.	0.91	0.90	0.95	0.96	0.96

The CFD model managed to predict the time variation of concentration with quite good accuracy, at least for the A and B experiments. The simulation of the third experiment depicted a significant deviation which must be attributed mainly to the strong-compared to the other cases- prevailing outdoor wind during this experiment. This fact reinforced infiltration inevitably. The last two simulations for the D and E experiment showed also an intense deviation. This can be attributed to the small deviation (1%) of the injection rate and partly to the infiltration which must not be negligible during these cases, as outdoor wind measurements revealed. Furthermore, the simplifications made for the determination of initial field of values of variables in every floor, contributed to the increase of the relative error for all runs. However, the model succeeded in predicting the trend of concentration evolution at all sampling points and for all experiments.

Figure 3 shows an example of this evolution as measured and as calculated during the experiment A and for the four floors.

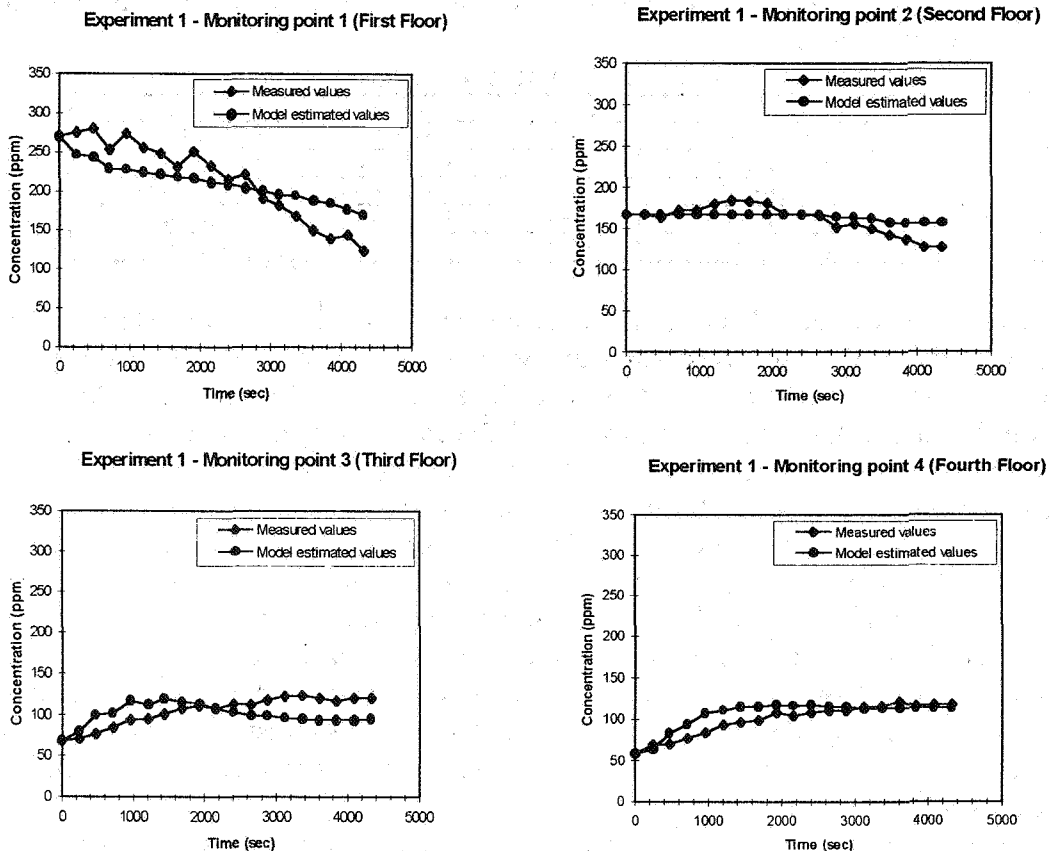


Figure 3. Measured and estimated concentration as a function of time ( experiment A)

Besides these problems that arose during the experiments, there are some other more basic difficulties. For instance, it must be noted, how difficult is to simulate full scale cases especially when this concerns quite large spaces. The detailed determination of thermal boundary conditions is very critical. This is very difficult when many surfaces with various thermal behavior exist, as in our case. In addition, in thermally-driven enclosures, a great difficulty comes from the turbulence models. These models are not strictly validated. Two different models usually show different results for the same configuration [19]. Much more experimental work is needed in order to better understand the phenomena and derive appropriate models for their description. Finally, the airflow through horizontal openings is physically highly transient, unstable and difficult to be described since it is driven by instability instead of a relatively stable distribution of pressure as through vertical openings.

## 5. Conclusions

A buoyancy-driven flow within the complex geometry of a stairwell was computed using Computational Fluid Dynamic simulation. Time-dependent computation revealed the airflow patterns which affects the contaminant transmission. The comparison between the experimental data and the estimations as mainly concern the time-dependent concentration evolution showed encouraging agreement despite the difficulties related with turbulence models, geometry, simplifications, experimental errors and boundary conditions.



Investigation of these factors is required so as to enhance the accuracy of this model. This fact will reinforce the already existing confidence for applying this computational model to further studies related to natural convection through horizontal openings. The final goal is to develop algorithms sufficient enough to be included in models using pressure networks so as to predict the interzone heat and mass transfer in the interior of multi-storey buildings.

## 6. References

1. Brown W G , 1962. " Natural convection through rectangular openings in partitions- 2 : Horizontal Partitions", *Int. J. Heat and Mass Transfer*, Vol 5, pp 869-881.
2. Reynolds A J , 1986. "The scaling of flows of energy and mass through stairwells" *Build. And Envir.* , Vol 21, No 314, pp 149-153.
3. Zohrabian A S , Mokhtarzadeh M R , Reynolds A J, 1989. "Buoyancy-driven air flow in a stairwell model with through -flow" *Brunel Univ., UK.*
4. Zohrabian A S , Mokhtarzadeh M R , Reynolds A J, 1988. "A numerical study of buoyancy-driven flows of mass and energy in a stairwell", 9<sup>th</sup> AIVC Conf. Gent, Belgium, pp.1-21.
5. Riffat S B , 1989. " A study of heat and mass transfer through a doorway in a traditionally built house ", *ASHRAE Trans.*, Vol 95, pp 584-589.
6. Riffat S B , Kohal J S , Shao L, 1994. " Measurement and CFD modelling of buoyancy-driven flows in horizontal openings " *Proc. ASHRAE IAQ94, Conf. Engineering Indoor Environment, St Louis.*
7. Ergin-Ozkan S, Mokhtarzadeh M R , Reynolds A J, 1992. "Two- and Three-dimensional finite volume predictions of flow in a stairwell and comparison with experiment" *Inter. Symposium on Room Air convection and ventilation eff., Tokyo.*
8. Haghghat, F., Jiang, Z., Wang, J.C.Y., 1989. "Natural convection and air flow pattern in a partitioned room with turbulent flow", *ASHRAE Trans. Vol 95, part 2, pp 155-161.*
9. Murakami, S., Kato, S. 1990. "Numerical and experimental study on flow and diffusion field in room, 11<sup>th</sup> AIVC Conf., Italy.
10. Alamdari F., Edwards S.C., Hammond, G.P., 1991. "Microclimate performance of an open atrium office building: a case study in thermo-fluid modeling. *IMechE*, pp 81-92.
11. Drangsholt F. 1993. "Air flow pattern and pollutant transmission in auditoria - measurements and CFD simulations". *Proc. 6<sup>th</sup> Conf. IAQ.*, Vol 5, pp 189-195.
12. Subrata R., Baker A.J. and Kelso R.M., 1993. "Airborne contaminant CFD modeling studies for two practical 3-D room air flow fields". *Proc. 6<sup>th</sup> Conf. IAQ*, Vol 5, pp 349-358
13. Markatos , N.C., Pericleous , K.A., 1984. "Laminar and turbulent natural convection in an enclosed cavity". *Int. J. Heat Mass Transfer*, Vol. 27 , No 5, pp 755-772.
14. Launder, B.E., and D.B. Spalding (1972) *Mathematical models of turbulence.* New York, Academic Press.
15. Beghein C., Allard F., Draoui A. 1992. " Numerical modeling of turbulent convection in athermally-driven square cavity". *Sem. 22 Procc. J.M. Burgers Centre.*
16. Lam C.K.G., Bremhost K., 1981. " A modified form of the k-ε model for predicting wall turbulence", *ASME J. Fluids Eng.*, Vol 103, p 456 .
17. Yap C., 1987. "Turbulent heat and momentum transfer in recirculating and impinging flows". *PhD Thesis, Faculty of Tech., Univ. of Manchester.*
18. Patankar, S.V (1980) *Numerical Heat Transfer and Fluid Flow*, Hemisphere, NY.